EURASIAN JOURNAL OF MATHEMATICAL AND COMPUTER APPLICATIONS
ISSN 2306–6172
Volume 13, Issue 3 (2025) 75 – 82

NUMERICAL SIMULATION OF HYDRATE SHELL GROWTH ON THE SURFACE OF GAS BUBBLE

Slastnaya D.A.[1], Vozhakov I.S., Sagidullin A.K., Bozhko Y.Y., Meleshkin A.V.

Abstract We present a mathematical model of hydrate shell growth on the surface of a HFC-134a bubble. The model is based on the assumption that the hydrate is a solid porous material. The change in the bubble radius and hydrate film thickness as a function of time was determined. It was revealed that hydrate shell growth occurs during the first three seconds, with the subsequent thickness of the hydrate shell remaining constant. This phenomenon is a result of pore blockage within the hydrate. The mathematical model was validated by experimental data.

Keywords: gas hydrates, hydrate shell, HFC-134a, numerical simulation

AMS Mathematics Subject Classification: 65Pxx

DOI: 10.32523/2306-6172-2025-13-3-75-82.

1 Introduction

Gas hydrates, also known as clathrate hydrates, are non-stoichiometric crystalline compounds [1, 2] that visually resemble ice. Hydrates are formed as a result of the interaction between water and a gas bubble under specific thermodynamic conditions. Any gas can act as a hydrate-forming gas, with the thermobaric conditions for hydrate stability being unique for the particular gas. The gas molecules are embedded in the crystal lattice formed by the water molecules and retained by van der Waals forces [3]. The formation of hydrates is a first-order phase transition, not a chemical reaction. Most gases form two basic types of hydrate unit cells. The cubic structure I [4, 5], comprising six large ($5^{12}6^2$) and two small cavities (5^{12}), is formed by gases such as CO, CH_4, H_2S, CO_2, SO_2, Xe, N_2O and others. The cubic structure II, comprising eight large cavities ($5^{12}6^4$) and 16 small cavities (5^{12}), is formed by SF_6, freons, C_3H_8, Ar, Kr, N_2, O_2 and other gases.

Gas hydrate studies have been attracting the attention of the global scientific community for a long time. The initial practical interest arose from the observation of parasitic gas hydrate formation at the sites of natural gas production and transportation in northern regions. As a result, the research on preventing and inhibiting gas hydrate formation started [6]. The discovery of gas hydrate deposits in permafrost zones and at ocean shelves also motivated further research. It was found that approximately 80% of the world's natural gas reserves are in hydrate form. Research on natural resource deposits primarily focuses on searching for and locating gas hydrate deposits and developing extraction methods for natural gas [7, 8].

Gas hydrates possess a multitude of advantageous properties that can be exploited in a variety of industrial applications. The capacity of gas hydrates to hold up to 170 volumes of natural gas enables them to be utilized for storing and transporting substantial quantities of gas. In contrast to liquefied gas, which requires maintaining a temperature of 111 K, gas hydrates can be transported at a temperature of 253 K, which significantly reduces energy

[1]Corresponding Author.

costs. Numerous research studies have focused on studying the dissociation of gas hydrates, with a specific emphasis on their combustion [9–12]. Another promising direction is the desalination of seawater and its purification from heavy metals and other harmful substances [13–16]. The gas hydrate structure is formed with only pure water, with H_2O drawn from the original solution during the hydrate formation process. In addition, during the formation of a hydrate it is possible to capture heavier gases by creating the necessary conditions for hydrate formation of these gases [17–19]. Gas hydrates can be used for multiple purposes, such as hydrogen storage, cold storage, food use, carbon dioxide sequestration, and many others [20–23].

Given the above, it is essential to prioritize research directions that involve determining thermodynamic conditions, examining the physical and technical properties of hydrates, and investigating the influence of catalysts and inhibitors on the hydrate formation process [24–27]. However, there is currently no economically feasible technology for hydrate production. Therefore, various approaches are being explored to accelerate the process, including the addition of promoters or physical manipulation of the reaction medium. Three main methods for exerting a physical influence on the hydrate formation process are the atomization of water in the atmosphere of a hydrate-forming gas, gas bubbling, and mechanical mixing of the medium.

Studies of hydrate shell morphology [28–30] have demonstrated that it is a solid porous material with a certain degree of strength [31]. The lateral growth of the hydrate shell is controlled by heat transfer processes [32–34]. However, once the hydrate shell completely covers the bubble surface, the hydrate effectively blocks the direct contact between the gas and liquid, slowing down and suppressing the mass transfer processes between the different phases. Therefore, the mass transfer of gas and liquid through the hydrate becomes the dominant process governing the lateral growth of the hydrate shell [35–37]. The growth rate of the hydrate shell is controlled simultaneously by three types of mass transfer processes: gas diffusion through the hydrate [38], water penetration through the pores hydrate due to capillary pressure [39], and gas dissolution in water. The process of hydrate formation involves the gradual compaction of the hydrate shell and the dynamic renewal of the hydrate structure. This process results in some pores being filled and channels clogged, leading to a decrease in the mass transfer of the shell [40].

A relationship between hydrate shell morphology, bubble hydrodynamics, and hydrate shell growth rate was revealed [41]. In addition, it is possible that the hydrate shell growth is associated not only with mass transfer processes but may depend on the hydrodynamics of the liquid phase and the thermodynamics of the system. The degree of supercooling, which varies depending on the environment (temperature and pressure) is a crucial parameter influencing both hydrate crystallization [35] and growth rate [28]. Generally, an increase in subcooling leads to a decrease in the mass transfer resistance within the hydrate shell, causing the hydrate shell to thicken more rapidly [42]. Furthermore, the growth of the hydrate shell is affected by the dynamics of the bubble, which is determined by gravity, buoyancy, and drag force. These, in turn, are a function of the geometry of the hydrate-covered bubble.

This paper presents a mathematical model for the growth of a hydrate shell on the surface of a HFC-134 bubble. The validity of the model was confirmed using experimental data. The paper is divided into several chapters, with Chapter 2 describing the experimental method for measuring the film thickness, Chapter 3 presenting the mathematical model, Chapter 4 discussing the results, and Chapter 5 summarizing the conclusions.

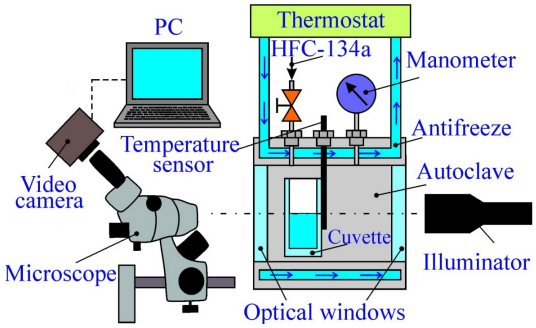

Figure 1: Schematic diagram of the experimental setup

2 Experimental methodology

The video recording of the formation of Freon 134a gas hydrate on the surface of the bubble released as a result of boiling of a drop of liquefied Freon was performed according to the procedure developed and described in [14]. We used a special optical cell, which is a thermostatically controlled autoclave with an internal volume of $22 - 25$ ml. Placed inside the autoclave was a glass cuvette of rectangular cross-section made of optical glass with overall dimensions $17\,\text{mm} \times 10\,\text{mm} \times 11\,\text{mm}$ (Fig. 1). The cuvette contained 1 mL of purified distilled water. At the ends of the working section of the unit, windows were installed to monitor and video record the processes taking place using an MBS-10 microscope and a TOUPCAM UCMOS 14000KPA video camera.

Once the cuvettes with purified water were placed into the high-pressure reactor, the autoclave was hermetically closed and subjected to a comprehensive purging process utilizing HFC-134a, with pressure gradually increased to 0.05 MPa. Following purging, the temperature within the autoclave working chamber was reduced to 283 K. Next, the internal volume of the reactor was filled with liquid HFC-134a, resulting in the formation of a hydrate that was subsequently melted. The melting of the resulting hydrate produced an emulsion on the surface of the water with small droplets of liquefied HFC-134a embedded in it. This emulsion functioned to immobilize the liquefied gas droplets, facilitating their visualization. The temperature of the working part of the autoclave was then reduced to 268.3 K. The choice of this temperature is due to the maximum supercooling of the medium relative to the hydrate stability line prior to the ice formation. As a result, the induction time was significantly reduced, as was the overall time of the experiment. The onset of gas hydrate film growth in the suspension initiated a thermal effect characterized by heat release during hydrate formation, subsequently causing droplet heating.

The droplets underwent heating and experienced a phase transition due to their small mass and the low thermal conductivity of the surrounding liquid. At the same time, the bubble that was released had a low growth rate, which prevented it from detaching from the drop (Fig. 2).

During the initial fractions of seconds, the surface of the bubble was transparent enabling the measurement of the bubble wall thickness. At the same time, a film of gas hydrate began

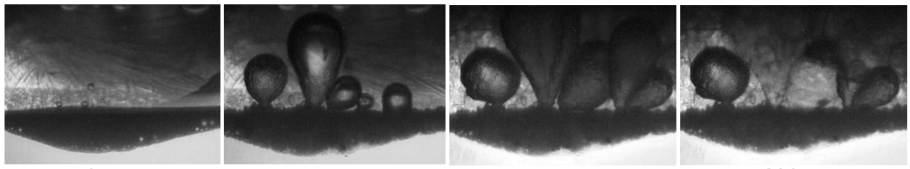

Figure 2: Released gas bubbles with hydrate shells growing on them at various time points

to grow almost immediately on the surface of the bubble, rendering it darker and hindering the assessment of crust thickness. The instantaneous growth of the hydrate film was due to the fact that the temperature inside the bubble had reached its maximum supercooling relative to the hydrate stability line, resulting from the gas temperature being equal to the saturation temperature at the current pressure in the system. Once the film growth stopped, the gas escaped due to deformation. The thickness of the remaining hydrate shell of the bubble was measured using a microscope, and the results were compared with the simulation data.

3 Mathematical model

Fig. 3 illustrates the process of hydrate formation on the surface of a gas bubble. The mathematical model is based on the assumption that the hydrate on the bubble surface is a thin, porous structure that allows for the simultaneous mass transfer of gas and liquid. The hydrate shell thickening is realized in two directions: at the liquid/hydrate interface and at the gas/hydrate interface. The formation of hydrate at the liquid/hydrate interface is controlled by the process of gas mass transfer through the hydrate. At the gas/hydrate interface, it is the rate of water penetration through the hydrate under the action of capillary pressure that serves to regulate the formation of hydrates.

The experiment described above reveals the rapid growth of hydrate on the surface of the bubble, which is due to the high solubility of gas in water at the two-phase interface. The growth continues for a few seconds, ultimately reaching a constant value. A sharp slowdown of hydrate shell growth is caused by the superposition of several factors. These are the thickening of the hydrate shell (formation and filling of pores), which impedes the diffusion of gas and

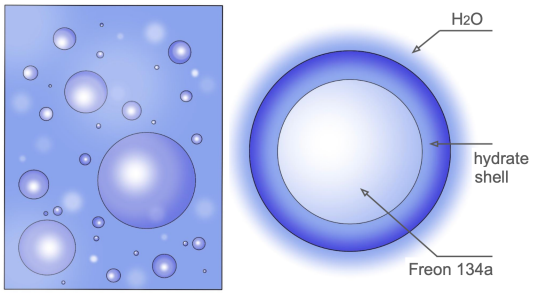

Figure 3: Schematic of hydrate shell growth on the bubble surface

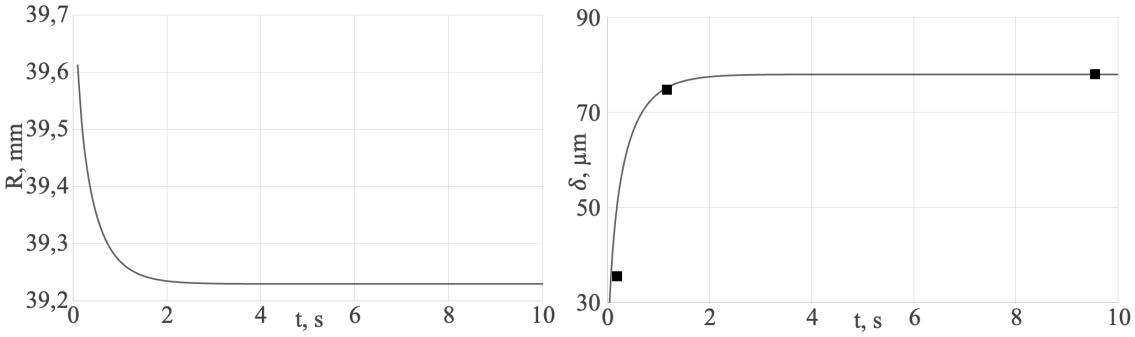

Figure 4: Variation of the radius (left) and thickness (right) of the hydrate shell, with the line representing the results of mathematical modeling and squares denoting the experimental values.

water through the hydrate layer, and a local increase in temperature of the hydrate surface area due to the exothermic process of hydrate formation. Earlier, the termination of hydrate growth was described by introducing an empirical function that controls the formation process and whose coefficients are taken from experimental data [43]. A similar approach was used in this study. We refined the mathematical model by introducing an empirical function $f(\delta, \delta_{max})$, which depends on the maximum hydrate shell thickness obtained in the experiment. This maximum value of hydrate shell thickness, denoted as δ_{max}, is equal to 78μm for the supercooling temperature of $\Delta T = 16\,\mathrm{K}$. As a result, the mathematical can be expressed as follows:

$$\frac{\partial R}{\partial t} = \frac{4}{3}\frac{\rho_w}{\rho_h}\frac{2\sigma r_c \phi f(\delta, \delta_{max})}{\eta_w \max(\delta, 10^{-6})} \tag{1}$$

$$\frac{\partial \delta}{\partial t} = \frac{4R}{(R+\delta)^2}\frac{\rho_w}{\rho_h}(D_h(1-\phi f(\delta, \delta_{max})) + D_w \phi f(\delta, \delta_{max})) - \frac{\partial R}{\partial t} \tag{2}$$

$$f(\delta, \delta_{max}) = 1 - \delta/\delta_{max}, \tag{3}$$

where R is the radius of the gas bubble, δ is the hydrate shell thickness, ρ_w is the density of water, ρ_h is the density of the hydrate, σ is the surface tension of water, r_c is the average radius of the pores in the hydrate, η_w is the dynamic viscosity of water, D_h is the diffusion coefficient of the gas in hydrate, and D_w is the diffusion coefficient of the gas in water.

The gas under consideration is HFC-134a, with a molar mass of 0.018 mol/kg and a density of 4.624 kg/m^3. The liquid under consideration is water, with a density of 999.79 kg/m^3 and a surface tension of 0.072 N/m. The density of the hydrate is 1047 kg/m^3 [44]. The diffusion coefficient of the gas through hydrate and liquid was calculated using the molecular model. The values obtained are $D_h = 9.2 \cdot 10^{-10}$ m^2/c, $D_w = 3.2 \cdot 10^{-9}$ m^2/c. The porosity of the hydrate shell was assumed to be constant, with the value taken from the previous work [45]. The initial gas bubble radius R_0 was set to 4 mm, and the initial hydrate shell thickness δ_0 was set to 1 μm The time step was set to 1 μs.

4 Results and Discussion

Fig. 4 illustrates the results of the simulation of the hydrate shell formation on the bubble surface compared to the experimental data. It should be noted that the radius of the bubble slightly decreased relative to the initial size, losing 0.4 mm but exhibiting stability. In other words, the formation of the hydrate shell itself does not lead to the collapse of the bubble. At the same time, the hydrate crust thickness increased 2.5 times from 30 μm to 80 μm in within approximately 3 seconds. The experimental study also demonstrated the hydrate shell thickness to be constant $\delta_{max} = 78\,\mu$m starting from the last measurement (t=9 s) for the duration of the remaining calculation period. This observation suggests that the cessation of the hydrate shell growth is not only due to the local heating and the system exiting the hydrate formation zone, given that cooling over time would lead to a resumption of growth. The discontinuation of hydrate growth may also be caused by the clogging of the hydrate pores, impeding the movement of water and gas through them from one surface to another. The data obtained are crucial for designing an enlarged reactor model for hydrate production. We suggest that by controlling the probability of hydrate formation on popping bubbles, one can limit the production cycle by accelerating the extraction of hydrated crystals from the reaction chamber.

5 Conclusion

This paper presents a numerical model of the hydrate shell on the surface of an HFC-134a bubble. The data obtained were validated by experimental results. The growth of the hydrate

shell was observed to occur during the first 3 seconds, with further exit to a constant value. The mathematical model that was developed in this study allows one to estimate the growth of a hydrate shell, providing a valuable tool for designing and operating reaction chambers utilized in the production of gas hydrates. The findings hold great importance in advancing the gas hydrate method for desalination and water purification, leading to enhanced production processes in the future.

Acknowledgement

The research is supported by RSCF (Project No. 22-79-10330), `https://rscf.ru/project/22-79-10330/`.
The software was provided by the Institute of Thermophysics under the state assignment for the IT SB RAS.

References

[1] Glew G., *Some effects of ionizing radiations on liquid whole milk and whey protein*, The International journal of applied radiation and isotopes, 6 (1959), 156-159.

[2] Yin Z. et al., *A review of gas hydrate growth kinetic models*, Chemical Engineering Journal, 342 (2018), 9-29.

[3] Krishna L., Koh C., *Inorganic and methane clathrates: Versatility of guest-host compounds for energy harvesting*, MRS Energy & Sustainability, 2 (2015), E8.

[4] Claussen W.F., Polglase M.F., *Solubilities and structures in aqueous aliphatic hydrocarbon solutions*, Journal of the American Chemical Society, 74 (1952), 4817-4819.

[5] Pauling L., Marsh R. E., *The structure of chlorine hydrate* , Proceedings of the National Academy of Sciences, 38 (1952), 112-118.

[6] Elhenawy S. et al., *Towards gas hydrate-free pipelines: a comprehensive review of gas hydrate inhibition techniques* , Energies, 15 (2022), 8551.

[7] Borodin S.L., Musakaev N.G., Belskikh D.S., *Mathematical modeling of a non-isothermal flow in a porous medium considering gas hydrate decomposition: A review*, Mathematics, 10 (2022), 4674.

[8] Khasanov M.K. et al., *Mathematical model of decomposition of methane hydrate during the injection of liquid carbon dioxide into a reservoir saturated with methane and its hydrate*, Mathematics, 8 (2020), 1482.

[9] Gaydukova O.S., Misyura S.Y., Strizhak P.A., *Investigating regularities of gas hydrate ignition on a heated surface: Experiments and modelling*, Combustion and Flame, 228 (2021), 78-88.

[10] Misyura S.Y. et al., *Combustion of a powder layer of methane hydrate: The influence of layer height and air velocity above the layer*, Flow, Turbulence and Combustion, 9 (2022), 175-191.

[11] Misyura S.Y. et al., *Studying the influence of key parameters on the methane hydrate dissociation in order to improve the storage efficiency*, Journal of Energy Storage, 44 (2021), 103288.

[12] Misyura S.Y. et al., *Gas hydrate combustion in five method of combustion organization*, Entropy, 22 (2020), 710.

[13] Meleshkin A.V. et al., *Phase Equilibrium for Hydrofluorocarbon R134a Hydrate. Hydrate-Based Desalination of NaCl Salt Solution* , Journal of Engineering Thermophysics, 33 (2024), 652-662.

[14] Misyura S.Y. et al., *The effect of various crystalline forms of HFC 134a hydrate on the growth rate and desalination efficiency* , Desalination, 586 (2024), 117903.

[15] Montazeri S.M., Kolliopoulos G., *Hydrate based desalination for sustainable water treatment: A review*, Desalination, 537 (2022), 115855.

[16] Zheng J. et al., *Progress and trends in hydrate based desalination (HBD) technology: A review*, Chinese Journal of Chemical Engineering, 27 (2019), 2037-2043.

[17] Strukov D.A. et al., *Study of the kinetics of methane-carbon dioxide exchange in gas hydrates below the ice melting point. Experimental data and computational model* , Thermochimica Acta, 736 (2024), 179737.

[18] Sergeeva M.S. et al., *Xenon recovery from natural gas by hybrid method based on gas hydrate crystallisation and membrane gas separation* , Journal of Natural Gas Science and Engineering, 86 (2021), 103740.

[19] Wang P. et al., *Review on the synergistic effect between metalPIP ,eЂњorganic frameworks and gas hydrates for CH_4 storage and CO_2 separation applications*, Renewable and Sustainable Energy Reviews, 167 (2022), 112807.

[20] Skiba S.S., Sagidullin A.K., Manakov A.Y., *Hydrogen solubility in gas hydrates with various auxiliary guests. Methane hydrate case study and comparison with the literature data*, International Journal of Hydrogen Energy, 51 (2024), 266-273.

[21] Sagidullin A.K., Manakov A.Y., *Growth Features of Gas Hydrate Films at Interface of Liquid Carbon Dioxide with Water and Sodium Dodecyl Sulfate Solution in Teflon and Steel Cuvettes*, Chemistry and Technology of Fuels and Oils, 59 (2024), 718-725.

[22] Misyura S. et al., *A Review of Gas Capture and Liquid Separation Technologies by CO2 Gas Hydrate*, Energies, 16 (2023), 3318.

[23] Zhdanov R.K. et al., *Accurate description of gas hydrates of carbon dioxide and hydrogen for storage and transportation* , Surfaces and Interfaces, 43 (2023), 103549.

[24] Bozhko Y.Y. et al., *Role of SiO_2 in the Formation of Hydrate Phases in the Presence of CH_4/CO_2*, Russian Journal of Inorganic Chemistry, 68 (2023), 233-237.

[25] Gets K.V. et al., *Theoretical Study of Formation of Hydrates from High-Concentration Metastable Solution of Carbon Dioxide in Water at Various Gas Concentrations*, Journal of Engineering Thermophysics, 32 (2023), 502-507.

[26] Bozhko Y.Y. et al., *Double Freon Hydrates: Composition and Thermodynamic Properties*, Journal of Engineering Thermophysics, 32 (2023), 62-68.

[27] Nesterov A.N. et al., *Promotion and inhibition of gas hydrate formation by oxide powders*, Journal of Molecular Liquids, 204 (2015), 118-125.

[28] Tanaka R., Sakemoto R., Ohmura R., *Crystal growth of clathrate hydrates formed at the interface of liquid water and gaseous methane, ethane, or propane: variations in crystal morphology*, Crystal Growth and Design, 9 (2009), 2529-2536.

[29] Li S.L. et al., *New observations and insights into the morphology and growth kinetics of hydrate films*, Scientific reports, 4 (2014), 4129.

[30] Ohmura R. et al., *Clathrate hydrate crystal growth in liquid water saturated with a guest substance: observations in a methane water system* , Crystal growth & design, 5 (2005), 953-957.

[31] Uchida T., Kawabata J., *Measurements of mechanical properties of the liquid CO_2-water-CO_2-hydrate system*, Energy, 22 (1997), 357-361.

[32] Mori Y.H., *Estimating the thickness of hydrate films from their lateral growth rates: application of a simplified heat transfer model*, Journal of crystal growth, 223 (2001), 206-212.

[33] Mochizuki T., Mori Y.H., *Clathrate-hydrate film growth along water/hydrate-former phase boundariesPIP ,eЂќnumerical heat-transfer study*, Journal of crystal growth, 290 (2006), 642-652.

[34] Peng B.Z. et al., *Hydrate film growth on the surface of a gas bubble suspended in water*, The Journal of Physical Chemistry, 111 (2007), 12485-12493.

[35] Sun C.Y. et al., *Studies on hydrate film growth*, Annual Reports Section "C"(Physical Chemistry), 106 (2010), 77-100.

[36] Shi B.H. et al., *An inward and outward natural gas hydrates growth shell model considering intrinsic kinetics, mass and heat transfer* , Chemical engineering journal, 171 (2011), 1308-1316.

[37] Lee J.D., Susilo R., Englezos P., *MethanePIP ,eЂњethane and methane-propane hydrate formation and decomposition on water droplets* , Chemical Engineering Science, 60 (2005), 4203-4212.

[38] Hirai S. et al., *MRI measurement of hydrate growth and an application to advanced CO_2 sequestration technology*, Annals of the New York Academy of Sciences, 912 (2000), 246-253.

[39] Mori Y.H., Mochizuki T., *Mass transport across clathrate hydrate films - a capillary permeation model*, Chemical engineering science, 52 (1997), 3613-3616.

[40] Davies S.R. et al., *In situ studies of the mass transfer mechanism across a methane hydrate film using high-resolution confocal Raman spectroscopy* , The Journal of Physical Chemistry C, 114 (2010), 1173-1180.

[41] Warzinski R.P. et al., *Dynamic morphology of gas hydrate on a methane bubble in water: Observations and new insights for hydrate film models*, Geophysical Research Letters, 41 (2014), 6841-6847.

[42] Taylor C.J. et al., *Macroscopic investigation of hydrate film growth at the hydrocarbon/water interface*, Chemical Engineering Science, 62 (2007), 6524-6533.

[43] Sun X. et al., *Modeling of dynamic hydrate shell growth on bubble surface considering multiple factor interactions*, Chemical Engineering Science, 331 (2018), 221-233.

[44] Jeong K. et al., *Tetrafluoroethane (R134a) hydrate formation within variable volume reactor accompanied by evaporation and condensation*, Review of Scientific Instruments, 86 (2015).

[45] Staykova D.K. et al., *Formation of porous gas hydrates from ice powders: diffraction experiments and multistage model*, The Journal of Physical Chemistry B, 107 (2003), 10299-10311.

Darya Slastnaya,
Institute of Thermophysics SB RAS,
Lavrentyev Av. 1, 630090 Novosibirsk, Russia,
Email: da.slastnaya@gmail.com,

Ivan Vozhakov,
Institute of Thermophysics SB RAS,
Lavrentyev Av. 1, 630090 Novosibirsk, Russia,
Email: vozhakov@gmail.com,

Aleksei Sagidullin,
Institute of Thermophysics SB RAS,
Lavrentyev Av. 1, 630090 Novosibirsk, Russia,
Nikolaev Institute of Inorganic Chemistry SB RAS,
Lavrentyev Av. 3, 630090 Novosibirsk, Russia,
Email: Sagidullin@niic.nsc.ru,

Yulia Bozhko,
Nikolaev Institute of Inorganic Chemistry SB RAS,
Lavrentyev Av. 3, 630090 Novosibirsk, Russia,
Email: bozhko@niic.nsc.ru,

Anton Meleshkin,
Institute of Thermophysics SB RAS,
Lavrentyev Av. 1, 630090 Novosibirsk, Russia,
Email: mav@itp.nsc.ru

Received 24.10.2024, Revised 11.11.2024, Accepted 06.12.2024, Available online 30.09.2025.